Far Eastern Studies Vol.7 May 2008
Center for Far Eastern Studies, University of Toyama

Physicochemical Environment of Formation of Tin Sulfide-Bearing Deposits in Japan

Masaaki Shimizu*, Marina Shimizu* and Kenro Tsunoda**

Abstract

Microscopic observations reveal that stannite formed at an earlier stage than stannoidite on the scale of polished sections, and this suggests that sulfur fugacity, $f(S_2)$, increased or that temperature decreased (or both) with the evolution of Sn mineralization. Concerning the $f(S_2)$ versus temperature range for the stannite-type deposits, at a given temperature, $f(S_2)$ increased from skarn deposits through Sn-W vein deposits to polymetallic vein deposits. Fe^{2+}/Zn ratios of coexisting stannoidite, sphalerite and tennantite-tetrahedrite from W-bearing polymetallic vein deposits were higher than those from W-free polymetallic vein deposits. This could imply that the W-bearing deposits formed under lower $f(S_2)$ or higher temperature conditions (or both) than the W-free deposits. The log $f(S_2)$ vs. temperature field of roquesite-bearing Sn ores from the Omodani and Akenobe deposits was superimposed to be approximately 10^{-6} atm. at 310 ℃ to 10^{-8} atm. at 285 ℃, in the same manner as that of the stannoidite-bearing ores.

Keywords *: stannite, stannoidite, roquesite, skarn deposits, polymetallic vein deposits, Sn-W vein deposits, epithermal deposits, stannite-type, stannoidite-type, temperature, sulfur fugacity.*

1. Introduction

Economic geology has a wide spectrum; targets for thorough investigation include not only ore deposits themselves but also all of the ore-forming processes, such as sources and channel ways of ore fluids, their reactions with host rocks, sources of the dissolved constituents, transportation by the fluids, and precipitation from fluids. Comprehensive genetic models for ore deposits can be obtained based on overall detailed geologic, alteration, fluid inclusion, stable isotope, and experimental studies. One example might be observing, describing and considering aggregates of ore minerals as the present status of our understanding of ores and ore deposits in terms of physicochemical environment of formation such as temperature, pressure, oxygen fugacity and sulfur fugacity, salinity, and on complexing.

Mineral resources have recently gained further their economic significance with their increasing consumption in our technologies. Rare metals such as Sn and In are linked to the growth of the computer, semiconductor and other industries; for example, In is now one of indispensable for the electrodes of liquid crystal displays even though its price has risen dramatically because of its insufficient availability.

This paper describes the environment of formation of and a genetic concept for Sn sulfide-bearing ore deposits in Japan. Since In mineralization has a high affinity for such Sn mineralization, it is also characterized.

* Department of Earth Sciences, Faculty of Science, University of Toyama, 3190 Gofuku, Toyama 930-8555, Japan.
E-mail: mshimizu@sci.u-toyama.ac.jp
** Faculty of Education and Human Sciences, University of Yamanashi, 4-4-37 Takeda, Kofu 400-8510, Japan.
E-mail: tkenro@yamanashi.ac.jp

2. Distribution of Sn Sulfide-Bearing Deposits in Japan

Tin sulfide-bearing deposits in Japan are generally grouped into skarn and vein deposits. The skarn deposits mean ore deposits genetically related to skarnization (mechanism for forming silicate minerals such as calcium-bearing amphibole, pyroxene, and garnet). The vein deposits mean ore deposits filling of faults or other fractures in host rocks in tabular or sheet-like form, and they are subdivided into three here: polymetallic, Sn-W, and epithermal.

The distribution of the Sn sulfide-bearing deposits in a so-called “mature”island arc system (Japan) is shown in Fig. 1. From the viewpoint of metallogenic epoch, these deposits are mainly divided into two groups: (1) Upper Cretaceous-Paleogene in age for backarc-side deposits about 300-400 km away from the axis of the present trench, and (2) Neogene in age for forarc-side deposits 200-300 km away from the trench axis.

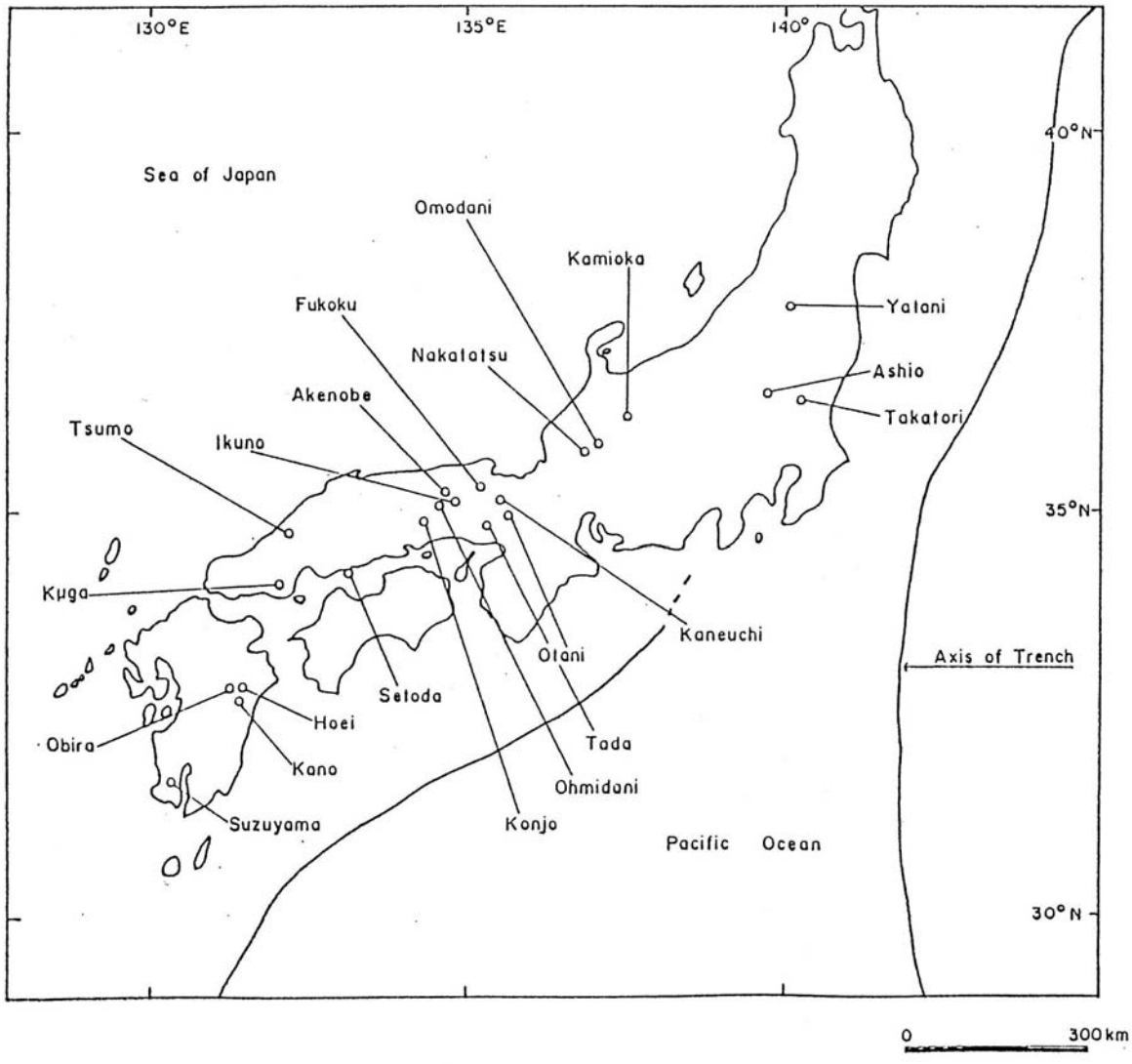

Figure 1 Map of Japan showing the distribution of Sn sulfide-bearing deposits studied.

Because stannite and stannoidite are rather common Sn sulfide minerals in the ore deposits associated with Sn mineralization, we propose that these deposits can be divided into two types—stannite type and stannoidite type—independent from the grouping of the metallogenic epoch. The stannite type, which means deposits where stannite occurs, consists of seven skarn deposits (Hoei, Nakatatsu, Obira, Kano, Kuga, Tsumo, and Kamioka), two polymetallic vein deposits (Akenobe and Ikuno), three Sn-W vein deposits (Ohtani, Kaneuchi, and Takatori) and an epithermal vein deposits (Yatani). The stannoidite type, which here means deposits where stannoidite occurs, is composed of eight polymetallic vein deposits (Tada, Ohmidani, Omodani, Akenobe, Fukoku, Setoda, Ikuno, and Konjo). Both stannite and stannoidite are observed, such as at Akenobe and Ikuno, but these two minerals are not recognized as forming simultaneously under the microscope. Such deposits are therefore classified into both stannite and stannoidite types.

3. Formation Temperature and Sulfur Fugacity of Stannite-Type Deposits

3-1. Iron and Zinc Partitioning between Coexisting Stannite and Sphalerite

Iron and zinc partitioning between coexisting stannite and sphalerite can be represented by the exchange reaction:

$$Cu_2FeSnS_4 \text{ (in stannite)} + ZnS \text{ (in sphalerite)} \Leftrightarrow Cu_2ZnSnS_4 \text{ (in stannite)} + FeS \text{ (in sphalerite)} \quad (1)$$

The partitioning coefficient (Kd) for the above reaction is represented by

$$Kd = \frac{X(Cu_2FeSnS_4)/X(Cu_2ZnSnS_4)_{stannite}}{X(FeS)/X(ZnS)_{sphalerite}} \quad (2)$$

In which X denotes the mole fraction of a given component in stannite or sphalerite.

Based on experimental studies, Nekrasov *et al.* (1979) and Nakamura and Shima (1982) reported a temperature dependency of iron and zinc partitioning between stannite and sphalerite.

$$\log Kd = 1.274 \times 10^3 \times T^{-1} - 1.174 \text{ (Nekrasov } et\ al.,\text{ 1979)} \quad (3)$$

$$\log Kd = 2.8 \times 10^{-3} \times T^{-1} - 3.5 \text{ (Nakamura and Shima, 1982)} \quad (4)$$

Both geothermometers are in agreement being close to 380 ℃ (Fig. 2); however, at the lower and higher temperatures the difference between the temperatures estimated from the equations (3) and (4) is larger.

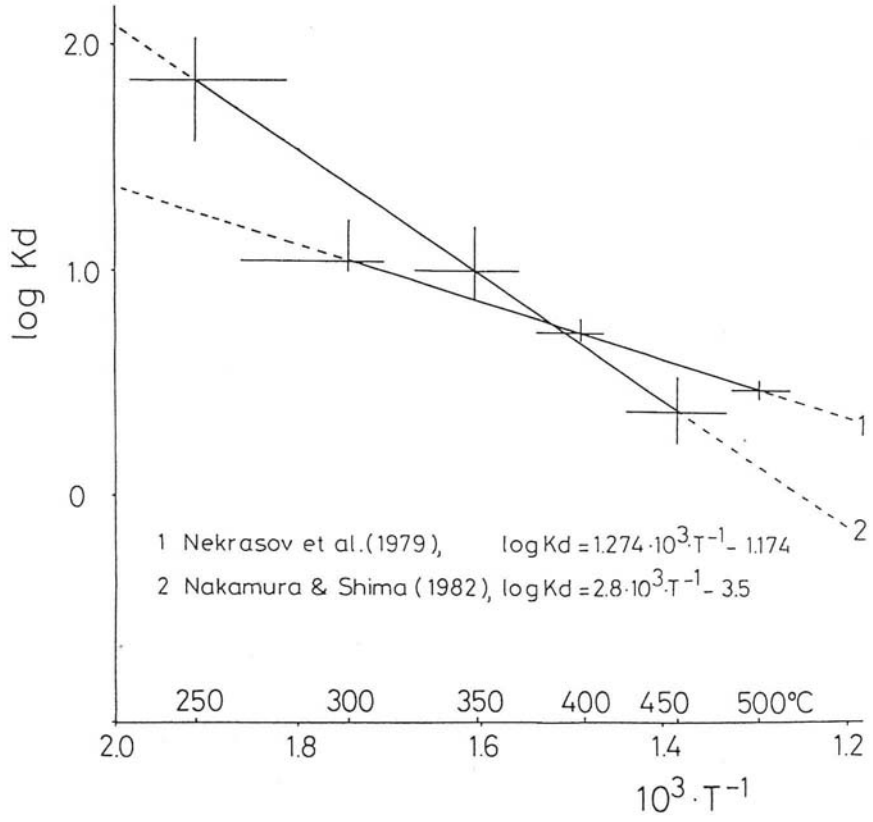

Figure 2. Comparison between the stannite-sphalerite geothermometer after Nekrasov *et al.* (1979) and that after Nakamura and Shima (1982). See equations (1) and (2) in the text. Cross bars indicate experimental uncertainties.

The chemical compositions of coexisting stannite and sphalerite were determined using an electron-microprobe analyzer (EPMA). Stannite and sphalerite are usually compositionally homogenous. Before the electron-microprobe analyses, the polished sections were carefully examined under the microscope. Some of them were abandoned after this check, because subsolidus phenomena and disequilibrium textures like stannite-chalcopyrite myrmekitic intergrowth were observed.

3-2. Comparison of Stannite-Sphalerite Temperatures with Filling Temperatures of Fluid Inclusions and Sulfur Isotope Temperatures

Figure 3 and Table 1 present a comparison between the stannite-sphalerite temperatures and filling temperatures of fluid inclusions or sulfur isotope temperatures. Data on the filling temperatures were obtained for the fluid inclusions in the quartz which precipitated at the same stage as that of the stannite-sphalerite pair. The sulfur isotope temperatures for the Nakatatsu deposit was analyzed for the galena-sphalerite pair which precipitated at the same stage as the stannite-sphalerite pair.

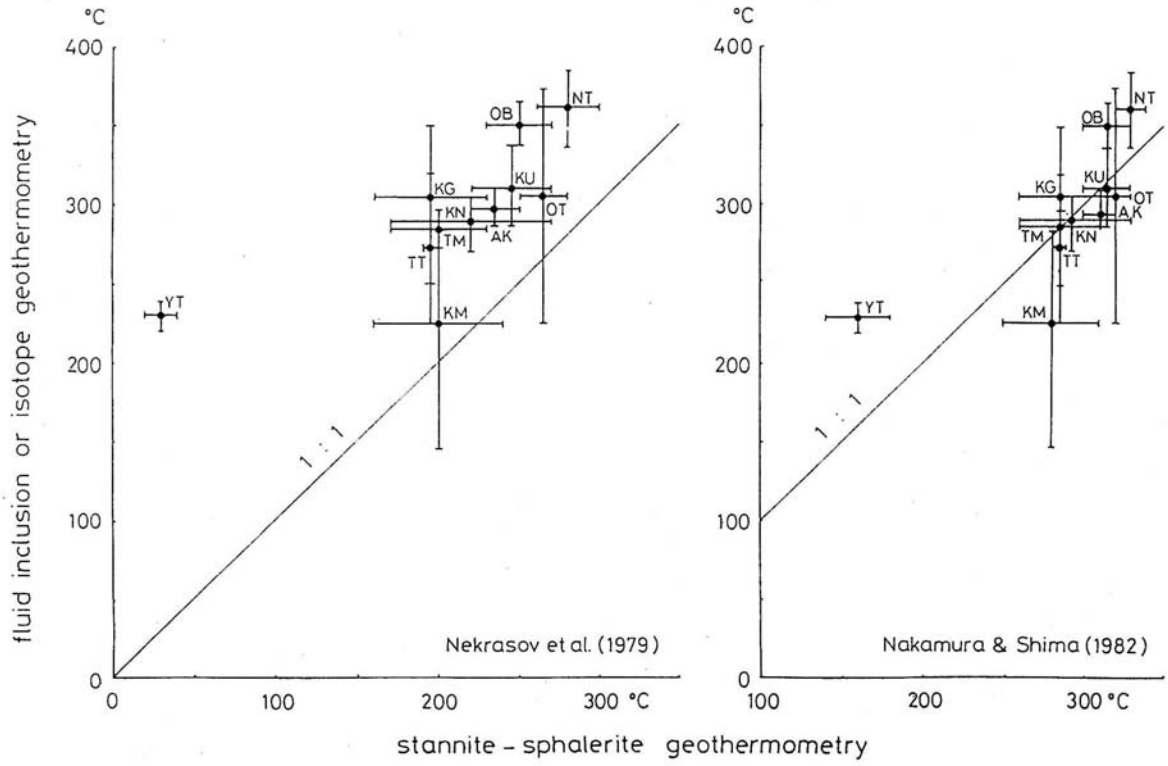

Figure 3. Comparison between the stannite-sphalerite geothermometer and filling temperatures of fluid inclusions or sulfur isotope temperatures.
Abbreviations, NT: Nakatatsu (Fukui Pref.), OB: Obira (Oita Pref.), KN: Kano (Miyazaki Pref.), KG: Kuga (Yamaguchi Pref.), TM: Tsumo (Shimane Pref.), KM: Kamioka (Gifu Pref.), OT: Ohtani (Kyoto Pref.), KU: Kaneuchi (Kyoto Pref.), AK: Akenobe (Hyogo Pref.), TT: Takatori (Ibaragi Pref.), YT: Yatani (Yamagata Pref.).

Table 1. Comparison between the stannite-sphalerite geothermometer and filling temperatures of fluid inclusions or sulfur isotope temperatures.

Sample Loc	Temp. (1)	Temp. (2)	I	II	Temp. (3)	Ref.
Hoei	350° – 320°	320° – 250°	0.30 – 0.34	3.29 – 5.41		
Nakatatsu	340° – 320°	300° – 260°	0.35 – 0.38	4.38 – 5.82	360° ± 25°	Shimizu & Iiyama (1982)[a]
Obira	330° – 300°	270° – 230°	0.25 – 0.29	4.31 – 5.67	365° – 336°	Nishio et al. (1953)
Kano	330° – 260°	270° – 170°	0.23 – 0.26	3.88 – 11.8	305° – 270°	Enjoji & Nedachi (1983)
Kuga	310° – 260°	230° – 160°	0.25 – 0.26	5.98 – 15.2	300° ± 50°	Takenouchi (1983)
Tsumo	310° – 260°	230° – 170°	0.14 – 0.25	3.11 – 12.6	297° – 273°	Enjoji & Shoji (1981)
Kamioka	310° – 250°	240° – 150°	0.22 – 0.23	4.71 – 15.1	284° – 145°	unpublished mine data
Ohtani	330° – 310°	280° – 250°	0.22 – 0.24	3.35 – 4.02	375° – 225°	Kim et al (1972)
Kaneuchi	330° – 300°	270° – 220°	0.20 – 0.23	3.32 – 5.10	337° – 286°	Kim et al. (1972)
Akenobe	320° – 300°	250° – 220°	0.10 – 0.13	2.39 – 2.48	310° – 285°	Shiozawa (1983)
Takatori	290° – 280°	200° – 190°	0.17	5.32 – 6.25	320° – 225°	Takenouchi & Imai (1971)
Ikuno	270° – 260°	180° – 170°	0.039 – 0.041	2.06 – 2.54		
Yatani	170° – 140°	40° – 20°	0.023 – 0.044	37.5	240° – 220°	unpublished Shikazono data
Daehwa	300° – 280°	220° – 200°	0.061 – 0.067	1.66 – 2.11		
East	270° – 260°	170°	0.081 – 0.082	4.01 – 4.34		
Cornwall	270° – 260°	180° – 170°	0.10	4.53 – 5.20		
Kuga	300° – 250°					Nakamura (1983)
Ohtani	340° – 240°					Nakamura (1983)
Suzuyama	300° – 250°					Urashima & Nedachi (1983)

Temp. (1): temperature based on Nakamura and Shima's geothermometer (°C)
Temp. (2): temperature based on Nekrasov et al.'s geothermometer (°C)
Temp. (3): temperature based on fluid inclusion or isotope [a] studies (°C)
I: (X_{FeS}/X_{ZnS}) in sphalerite
II: $(X_{Cu_2FeSnS_4}/X_{Cu_2ZnSnS_4})$ in stannite

Figure 3 reveals that Nakamura and Shima's geothermometer would be rather consistent with the temperatures estimated based on the fluid inclusion or sulfur isotope studies. It is also notable that almost all stannite-sphalerite temperatures are within ±30 ℃ of average filling temperatures and sulfur isotope temperatures.

3-3. Formation Temperature and Sulfur Fugacity of Stannite-Type Deposits

The temperatures estimated based on equation (4) range from about 350 to 250 ℃ for both skarn and vein deposits except for the Yatani epithermal Au-Ag vein deposit (Table 1).

The chemical compositions of the coexisting stannite and sphalerite are plotted on log $(X_{FeS}/X_{ZnS})_{sphalerite}$ vs. log $(X_{Cu_2FeSnS_4}/X_{Cu_2ZnSnS_4})_{stannite}$ diagrams (Figs. 4 and 5). Iso- log sulfur fugacity ($f(S_2)$) lines are based on Nakamura and Shima's equation and thermochemical data on the Fe-Zn-S system by Scott and Barnes (1971). The line representing 20.8 mol.% FeS in sphalerite, which corresponds to the composition of sphalerite in equilibrium with pyrite and pyrrhotite at 1 bar as determined by Boorman (1967), is also given on the diagram. It is evident in Figs. 4 and 5 that the FeS content of sphalerite coexisting with pyrite is generally lower than that of sphalerite coexisting with pyrrhotite or both pyrite and pyrrhotite.

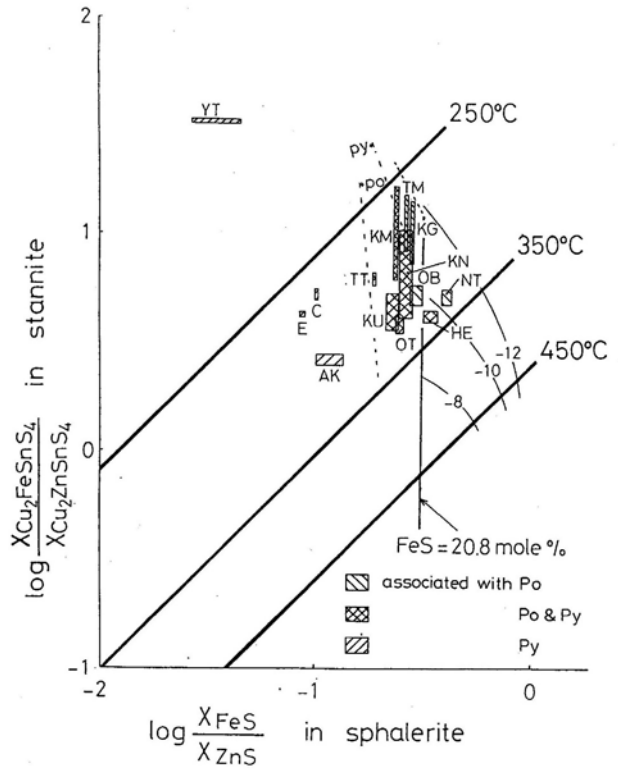

Figure 4. Diagram of log $(X_{FeS}/X_{ZnS})_{sphalerite}$ vs. log $(X_{Cu_2FeSnS_4}/X_{Cu_2ZnSnS_4})_{stannite}$ showing that sphalerite and stannite are associated with pyrrhotite (Po) and/or pyrite (Py). Temperature lines are based on data by Nakamura and Shima (1982). Solid curves show log $f(S_2)$ based on data by Scott and Barnes (1971) in the pyrrhotite field. Abbreviations are the same as Fig. 3 and He: Hoei (Oita Pref.), C: Cornwall (Penn., U.S.A.), East (Cornwall, U.K.).

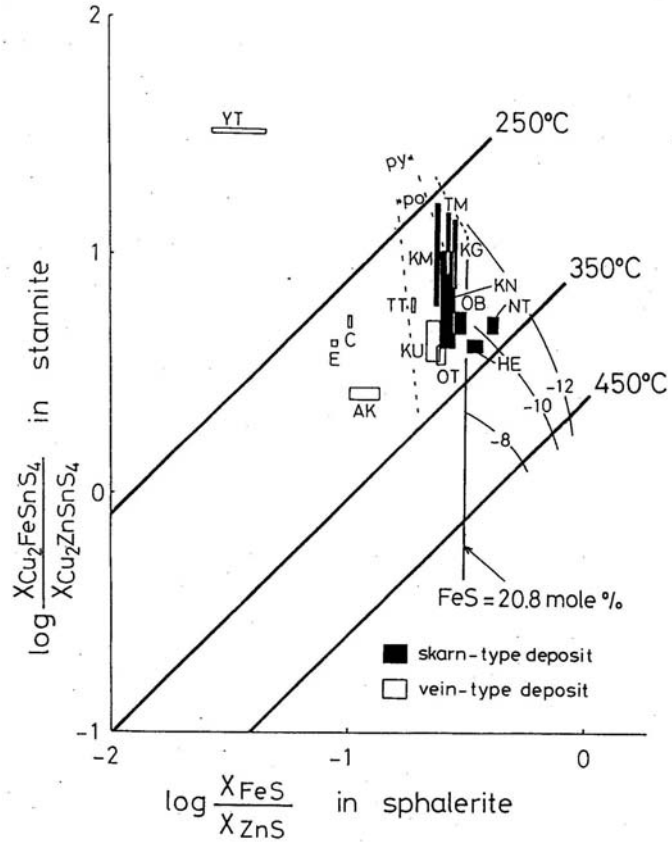

Figure 5. Diagram of log $(X_{FeS}/X_{ZnS})_{sphalerite}$ vs. log $(X_{Cu_2FeSnS_4}/X_{Cu_2ZnSnS_4})_{stannite}$ showing each deposit is skarn or vein.

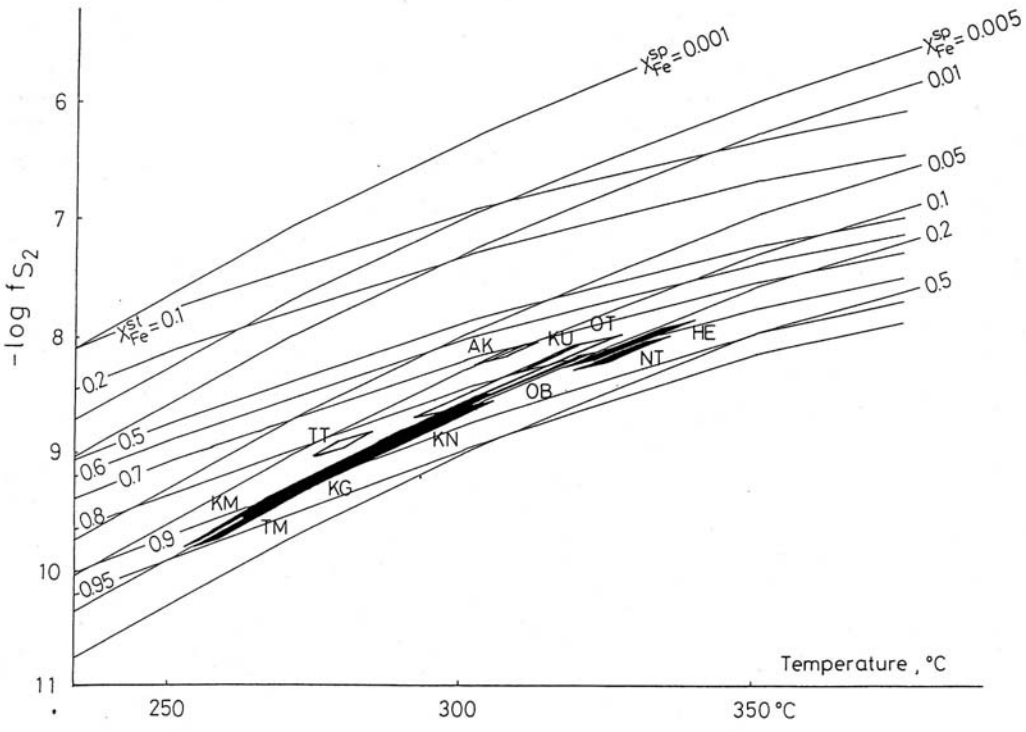

Figure 6.. Temperature vs. log $f(S_2)$ diagram. Skarn deposits (solid squares) are considered to be formed under lower $f(S_2)$ condition than vein deposits (open squares).

Iso-FeS content lines for sphalerite in equilibrium with pyrite or pyrrhotite were drawn on the log $f(S_2)$ vs. temperature diagram (Fig. 6) using thermochemical data reported by Scott and Barnes (1971) and Barton and Skinner (1979). The relation between the iron contents of stannite in equilibrium with sphalerite and pyrite or with sphalerite and pyrrhotite was derived based on thermochemical data reported by Scott and Barnes (1971), Barton and Skinner (1979) and Nakamura and Shima (1982) (Fig. 6).

Consequently, concerning the $f(S_2)$ vs. temperature range for the stannite-type deposits, at a given temperature, $f(S_2)$ increases from the skarn deposits through Sn-W vein deposits to polymetallic vein deposits.

4. Formation Temperature and Sulfur Fugacity of Stannoidite-bearing Sn Ores

4-1. Textures and Mineral Assemblages of Stannoidite-Bearing Sn Ores

Two characteristic textures of stannoidite-bearing ores are generally observed under the microscope. Where relic cassiterite remains, such as observed in the ores from the Konjo and Ashio deposits, stannoidite usually includes stannite, and stannite in turn includes aggregates of cassiterite grains (Fig. 7). This texture suggests the following sequence of precipitation of these Sn minerals: cassiterite (early) → stannite → stannoidite (late).

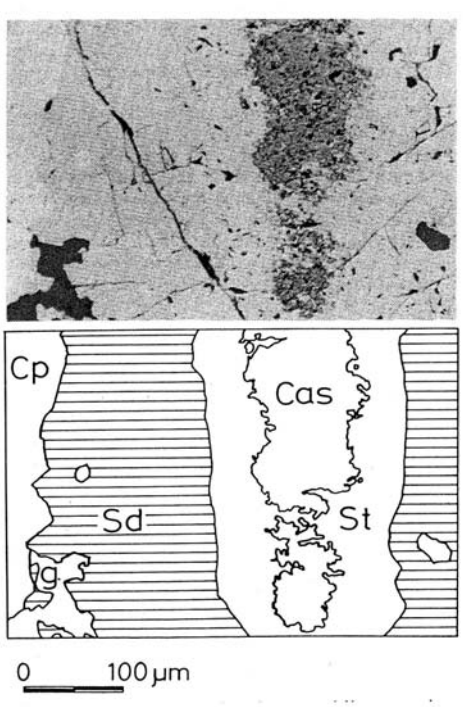

Figure 7. Photomicrograph of stannoidite-stannite-cassiterite-bearing sample from the Konjo ore deposit (Okayama Pref.). Abbreviations, Sd: stannoidite, St: stannite, Cp: chalcopyrite, Cas: cassiterite (SnO_2).

On the other hand, where mawsonite occurs at the margin of some stannoidite grains, such as observed in the samples from the Tada, Ohmidani, Omodani and Fukoku deposits, mawsonite shows a replacement or reaction texture (Fig. 8). In this case, stannite is invariably absent. This texture suggests the following sequence of precipitation: stannoidite → mawsonite.

The sequence of precipitation of Sn minerals inferred from the two characteristic textures might be: cassiterite → stannite → stannoidite → mawsonite.

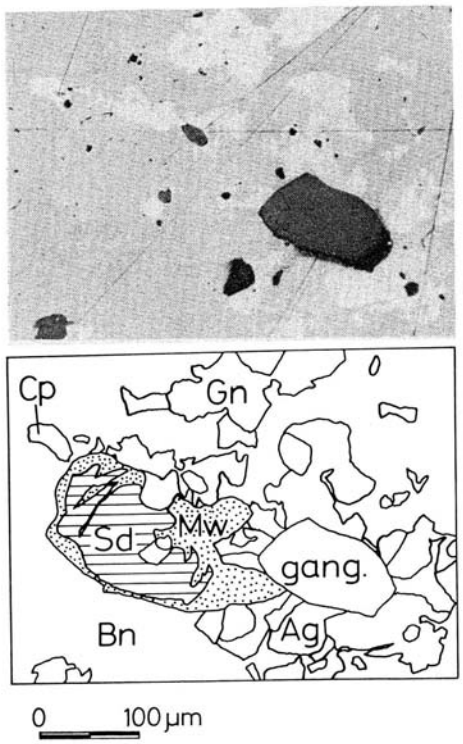

Figure 8. Photomicrograph of stannoidite-mawsonite-bornite-bearing sample from the Tada ore deposit (Hyogo Pref.). Abbreviations, Mw: mawsonite, Bn: bornite, Cp: chalcopyrite, Gn: galena, Ag: Ag minerals, gang.: gangue minerals.

The common opaque minerals that coexist with stannoidite are chalcopyrite, bornite, sphalerite, tennantite-tetrahedrite-series minerals and roquesite: these seem to have formed nearly contemporaneously, and this assemblage generally does not include stannite. It is also noteworthy that stannoidite does not coexist with pyrite except in the Sn ores from the Ashio deposit which contain stannite together with stannoidite. But stannite coexists with pyrite.

4-2. Formation Temperature and Sulfur Fugacity of Stannoidite-type Deposits

Many analytical data obtained with an EPMA reveal that most of the stannoidite, sphalerite and tennantite-tetrahedrite grains are compositionally homogeneous. Ranges of atomic Fe^{2+}/Zn ratios of coexisting stannoidite, sphalerite and tennantite-tetrahedrite from Japanese Sn-bearing vein deposits are summarized in Table 2. The atomic Fe^{2+}/Zn ratio of stannoidite was calculated from the total Fe/Zn ratio obtained by the electron-microprobe analysis and is based on the relationship:

$$(Fe^{2+}/Zn)_{stannoidite} = 1/3\{(\text{total Fe/Zn}) - 2\} \quad (5)$$

A continuous solid solution is inferred to exist between $Cu_8Fe^{2+}Fe^{3+}{}_2Sn_2S_{12}$ (ideal stannoidite) and $Cu_8ZnFe^{3+}{}_2Sn_2S_{12}$ ("zinc-stannoidite"), and the Fe^{2+}/Zn ratio of stannoidite is positively correlated to that of sphalerite and that of tennantite-tetrahedrite. No experimental data for temperature dependency of iron and zinc partitioning among these minerals have yet been obtained, but they could be of use as geothermometers in the future.

Table 2. Atomic Fe^{2+}/Zn^{2+} ratio of coexisting stannoidite (Sd), sphalerite (Sp) and tennnite-tetrahedrite-series minerals (Tenn).

Ore Dep.	Sd (avg: no. analysis)	Sp (avg: no. analysis)		Tenn (avg: no. analysis)
Tada	0.01 - 0.14 (0.08: 9)	0.002 - 0.007 (0.004: 8)	↑	absent
Ohmidani	0.09 - 0.14 (0.12: 7)	absent	Sp dominant	0.09 - 0.19 (0.14: 5)
Omodani	0.11 - 0.32 (0.22: 9)	0.004 - 0.011 (0.007: 8)		0.22 - 0.24 (0.23: 2)
Akenobe*	0.38 - 0.43 (0.41: 2)	0.005 - 0.008 (0.006: 3)		0.12 - 0.23 (0.18: 5)
Fukoku	0.11 - 0.72 (0.46: 9)	0.015 (0.015: 1)		0.94 - 1.61 (1.14: 4)
Ashio	0.58 - 1.19 (0.87: 3)	0.036 - 0.041 (0.039: 2)		0.34 - 3.97 (1.25: 4)
Setoda	1.06 - 1.43 (1.21: 9)	absent		absent
Ikuno	1.31 - 1.41 (1.38: 6)	absent		1.13 - 3.02 (1.90:11)
Konjo	2.01 - 2.10 (2.05: 6)	absent		1.52 - 4.38 (2.77: 7)

* Shiozawa (1984)

Table 3. Fe/Zn ratio of sphalerite from Sn-bearing vein deposits in Japan.

Ore Dep.	Fe/Zn
Sphalerite + stannoidite	
Tada	0.002 - 0.007
Omodani	0.004 - 0.011
Akenobe	0.005 - 0.008
Fukoku	0.015
Sphalerite + stannoidite + stannite	
Ashio	0.036 - 0.041
Sphalerite + stannite (Shimizu & Shikazono 1985)	
Yatani	0.023 - 0.044
Ikuno	0.039 - 0.041
Akenobe	0.10 - 0.13
Takatori	0.17
Kaneuchi	0.20 - 0.23
Ohtani	0.22 - 0.24

The Fe/Zn ratio of sphalerite coexisting with stannite or stannoidite is listed in Table 3. Note that the iron content of sphalerite coexisting with stannoidite is very low, compared with that of sphalerite with stannite.

Based on coexisting stannoidite, sphalerite, chalcopyrite and bornite, the following chemical reaction can be used to estimate $f(S_2)$ of the formation of the mineral assemblage.

$$5CuFeS_2 = Cu_5FeS_4 + 4(FeS)_{sp} + S_2 \qquad (6)$$

in which $(FeS)_{sp}$ denotes the FeS component in sphalerite. The equilibrium constant for reaction (6) is expressed as

$$K = a^{sp}_{FeS} \cdot f(S_2) \qquad (7)$$

The free energy of the reaction (6) is expressed as

$$\Delta G_r = - RT \ln K = - RT \ln \{ a^{sp}_{FeS} \cdot f(S_2)\} \qquad (8)$$

Therefore, $f(S_2)$ in logarithmic units is represented as

$$\log f(S_2) = - \Delta G_r / 4.575T - \log a^{sp}_{FeS} \qquad (9)$$

The free energy of reaction (6), ΔG_r, as a function of temperature can be derived from the thermochemical data for the chalcopyrite-bornite-pyrite-S_2 (gas) equilibrium (Schneeberg, 1973)

and FeS-pyrite-S_2 (gas) equilibrium (Barton and Skinner, 1979). The activity coefficient of FeS in sphalerite is assumed to be 2.4, from the experimental data reported by Barton and Toulmin (1966).

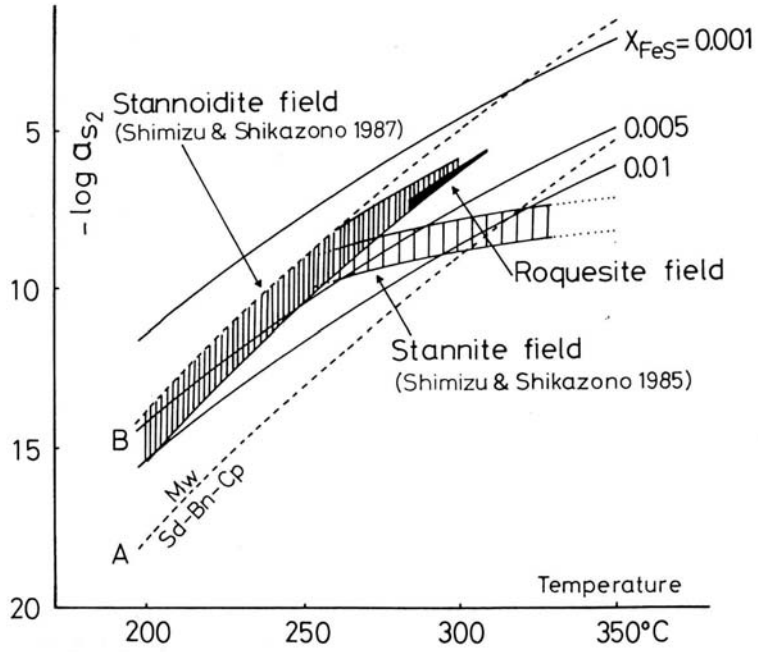

Figure 9. Temperature vs. log a(S_2) diagram for roquesite-bearing ores. Curves A and B correspond to a(S_2) vs. temperature relationships for the assemblage of stannoidite-chalcopyrite-bornite-mawsonite-S_2 (gas) for a(Fe) = 1 and a(Fe) = 0.1. Here, a(Fe) is defined as the activity of the $Cu_8Fe^{3+}{}_2Fe^{2+}Sn_2S_{12}$ component in the stannoidite solid solution. Abbreviation, Mw: mawsonite, Sd: stannoidite, Bn: bornite, Cp: chalcopyrite.

The relationship between temperature and FeS content of sphalerite in equilibrium with bornite and chalcopyrite was obtained on the basis of this equation (9). Isopleths for the FeS content of sphalerite in equilibrium with chalcopyrite and bornite were drawn on a log f(S_2) vs. temperature diagram (Fig. 9). As summarized in Fig. 9 and Table 3, sphalerite coexisting with stannoidite contains a mole fraction of a stannoidite-bearing assemblage and can not be estimated precisely, but fluid inclusion studies of the Sn-bearing vein deposits in Japan considered here (e.g., Imai, 1973) suggest that a stannoidite-bearing assemblage formed in the temperature range from 300 to 200 ℃. Accepting this temperature range, we estimated the probable f(S_2) region for the stannoidite-bearing assemblage (Fig. 9).

Lee *et al.* (1975) conducted an experimental study on the equilibrium for the assemblage of stannoidite-chalcopyrite-bornite-mawsonite-S_2 (gas) in the temperature range from 430 to 300 ℃. Curves A and B in Fig. 9 correspond to the f(S_2) vs. temperature relationship for this equilibrium assemblage for a_{Fe} = 1 and a_{Fe} = 0.1, respectively, in which a_{Fe} is defined as the activity of the $Cu_8Fe^{2+}Fe^{3+}{}_2Sn_2S_{12}$ component in stannoidite solid-solution.

The uncertainty in f(S_2) for this assemblage at constant temperature, as deduced from the experimental studies by Lee *et al.* (1975), increases with decreasing temperature. At 300 ℃ the uncertainty may be ±0.5 log f(S_2). Therefore, the f(S_2) estimated from this assemblage for a

temperature below 300 ℃ (in which range experimental studies have not been performed) might be large, probably more than ±0.5 log $f(S_2)$. Unfortunately, we can not estimate $f(S_2)$ and the temperature from the assemblage because a relevant experimental studies have not been carried out at temperatures below 300 ℃, and no information about the thermochemical mixing-properties of the stannoidite solid-solution is available. But note that theoretically it would be possible to estimate both $f(S_2)$ and the temperature based on the stannoidite-mawsonite-bornite-chalcopyrite-sphalerite assemblage if reliable experimental data on the assemblage and analytical data on sphalerite and stannoidite of the assemblage were available.

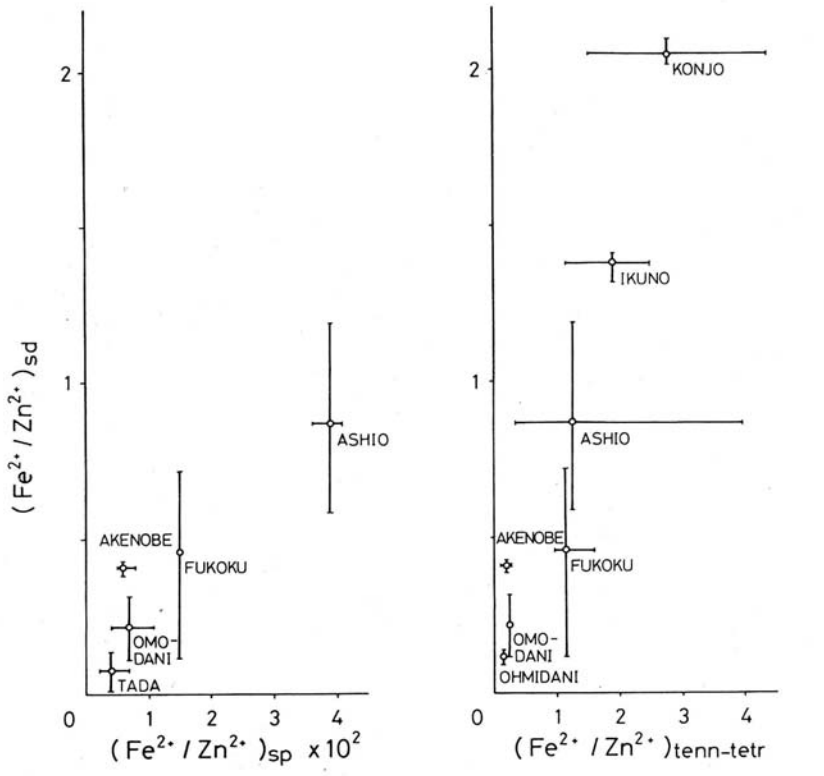

Figure 10. Fe^{2+}/Zn^{2+} of sphalerite (left) and of tennnite-tetrahedrite-series minerals (right) as a function of Fe^{2+}/Zn^{2+} of stannoidite (atomic proportions.)

As shown in Fig. 10 and Table 2, the Fe^{2+}/Zn ratio of coexisting stannoidite, sphalerite and tennantite-tetrahedrite from the Tada, Omodani and Ohmidani deposits are low, compared with those from other deposits such as the Ashio, Akenobe and Ikuno deposits. The former three are characterized by Zn-dominant polymetallic (Zn-Cu-Ag-Au) mineralization and W was not recovered, whereas the latter three are characterized by Cu-dominant polymetallic (Cu-Zn-Pb-Sn-W-Ag-Au-Bi) mineralization and W was recovered.

The Fe/Zn ratios of coexisting stannoidite, sphalerite and tennantite-tetrahedrite from W-bearing polymetallic vein deposits are higher than those from W-free polymetallic vein deposits. This could imply that the W-bearing deposits formed under lower $f(S_2)$ or higher temperature conditions (or both) than the W-free deposits.

4-3. Environment of formation of stannite- and stannoidite-type vein deposits

The estimated $f(S_2)$ vs. temperature ranges for formation of stannite- and stannoidite-bearing assemblages from the vein deposits are shown in Fig. 9, based on the thermochemical data on the mineral assemblage, FeS contents of sphalerite and fluid inclusion data. As mentioned above, microscopic observations reveal that stannite formed at an earlier stage than stannoidite on the scale of polished sections, and this suggests that $f(S_2)$ increased or that temperature decreased (or both) with the evolution of Sn mineralization.

5. Application to Roquesite-Bearing Sn Ores

After the first report of the occurrence of roquesite ($CuInS_2$, In analogue of chalcopyrite) in Japan by Kato and Shinohara (1968), Shimizu and Kato (1991) documented new occurrences of roquesite in Sn ores of four Japanese polymetallic vein deposits which show nearly the same mineral assemblages. The information on possible $f(S_2)$ and the temperature of the formation of In-bearing Sn mineralization can be estimated.

Table 4. Mineral assemblage in specimens studied and range of (atomic) Fe^{2+}/Zn.

Ore Deposit	Sp	Tn-Td	Bn	Rq	Sd	Cp	Others
Omodani	++	++	++	+	+	+	Lo,Ap,Mw,Gn,Ag
Fe^{2+}/Zn	0.005**	0.28-0.37			0.07-0.32		
max. wt.% In (*)	0.83 (16)	0.07 (19)	0.02 (62)	(8)	0.09 (10)	0.09 (13)	
Akenobe	++	++	+	+	++	+	Mw,Gn
Fe^{2+}/Zn	0.003-0.005	0.03-0.12			0.05-0.38		
max. wt.% In (*)	0.48 (9)	0.05 (19)	0.03 (9)	(10)	0.11 (11)	0.08 (8)	
Fukoku	++	+		+	++	+	Mw,Md
Fe^{2+}/Zn	0.004-0.015	0.88-1.25			0.45-0.72		
max. wt.% In (*)	0.08 (20)	0.98 (12)		(6)	0.30 (14)	0.21 (33)	
Ikuno	+	+		+	++	+	Ap,Gn
Fe^{2+}/Zn	0.016-0.036	1.65-2.00			0.97-1.49		
max. wt.% In (*)	1.61 (7)	0.09 (10)		(15)	0.13 (23)	0.31 (35)	

Abbreviations: Ag native silver, Ap arsenopyrite, Bn bornite, Cp chalcopyrite, Gn galena, Lo löllingite, Md matildite, Mw mawsonite, Rq roquesite, Sd stannoidite, Sp sphalerite, Tn-Td tennantite-tetrahedrite ++ common, + less common.

*) number of analysis

**) sphalerite poorest in Cu; there are many tiny chalcopyrite inclusions in sphalerite.

Mineral assemblages of the specimen studies and ranges of atomic Fe^{2+}/Zn ratios are summarized in Table 4. There is a wide range of Fe^{2+}-for-Zn substitution in coexisting stannoidite, sphalerite and tennantite-tetrahedrite. The comparison of estimated temperatures of formation of roquesite-bearing ores from the geological standpoint enables the four deposits in Table 4 to be grouped into two pairs: Ikuno-Fukoku and Akenobe-Omodani; the estimated temperature of the formation of the former is higher than that of the latter.

The In contents of sphalerite, tennantite-tetrahedite, stannoidite and chalcopyrite from the Ikuno and Fukoku deposits generally tend to be higher than those from the Omodani and Akenobe deposits (Table 4). The high In contents of these minerals probably arise from the high temperature of the formation, provided that the In concentrations in all the deposits was approximately equal.

Filling temperatures of fluid inclusions in the coexisting quartz from the Omodani and Akenobe deposits give a temperature ranging from 310 to 285 ℃ (Fig. 11).

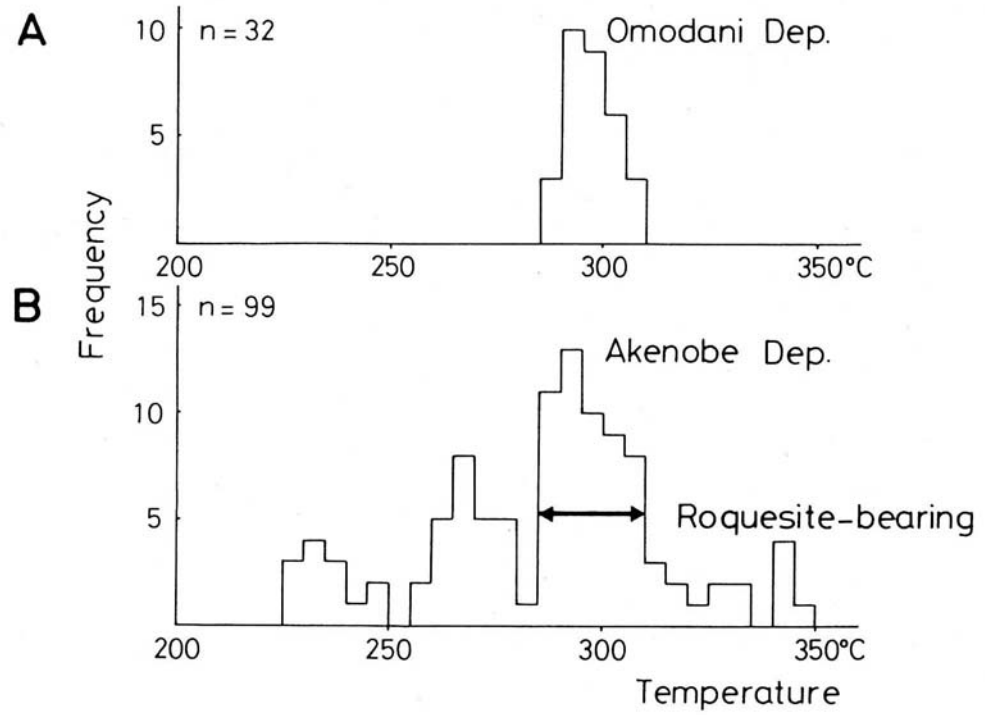

Figure 11. Histograms of filling temperatures of fluid inclusions in quartz associated with roquesite from the Omodani ore deposit (A) and Chiemon No. 4 vein, Akenobe ore deposit (B).

In Fig. 9, the log $f(S_2)$ vs. temperature field of the roquesite-bearing Sn ores from the Omodani and Akenobe deposits is superimposed to be approximately 10^{-6} atm. at 310 ℃ to 10^{-8} atm. at 285 ℃, in the same manner as that of the stannoidite-bearing ores.

The isotopic composition of sulfur in the Akenobe and Ikuno deposits were reported by Yamamoto (1974), Sasaki and Ishihara (1980) and Ishihara *et al.* (1981), but those of roquesite-bearing ores were not reported. It is noteworthy that a preliminary S isotope study on the roquesite-bearing ores indicates a very narrow range of $\delta^{34}S$ values from -0.9 to +0.3 ‰ (Table 5). This could indicate a magmatic origin and suggest either that the physicochemical environment of the deposits did not change during the In mineralization or that the metal/sulfur ratios in the ore fluids responsible for the In mineralization were too small to change the isotopic compositions in the fluids significantly.

Table 5. Sulfur isotopic compositions of roquesite-bearing bulk ores.

Ore Deposit	$\delta^{34}S$ (per mil)
Omodani	-0.8
Akenobe	-0.9 (average, n=32)*
Fukoku	-0.5
Ikuno	+0.3

*) Shiozawa's unpublished data

6. Summary

(1) Microscopic observations reveal that stannite formed at an earlier stage than stannoidite on the scale of polished sections, and this suggests that $f(S_2)$ increased or that temperature decreased (or both) with the evolution of Sn mineralization.
(2) Concerning the $f(S_2)$ vs. temperature range for the stannite-type deposits, at a given temperature, $f(S_2)$ increased from the skarn deposits through Sn-W vein deposits to polymetallic vein deposits.
(3) Fe/Zn ratios of coexisting stannoidite, sphalerite and tennantite-tetrahedrite from W-bearing polymetallic vein deposits were higher than those from W-free polymetallic vein deposits. This could imply that the W-bearing deposits formed under lower $f(S_2)$ or higher temperature conditions (or both) than the W-free deposits.
(4) The log $f(S_2)$ vs. temperature field of the roquesite-bearing Sn ores from the Omodani and Akenobe deposits was superimposed to be approximately 10^{-6} atm. at 310 ℃ to 10^{-8} atm. at 285 ℃, in the same manner as that of the stannoidite-bearing ores.

Acknowledgments

We sincerely thank Professor Kunio Kawada and Professor Naoya Wada, the Center for Far Eastern Studies, University of Toyama, for their helpful advice during our study. We are also grateful to two anonymous referees for their comments, which enable us to improve the manuscript.

References

Barton, P. B. Jr. and Skinner, B. J., 1979. Sulfide mineral stabilities. *In* Geochemistry of Hydrothermal Ore Deposits, 2nd Ed., H. L. Barnes ed., 278-403, Wiley-Interscience, New York.

Barton, P. B. Jr. and Toulmin, P., III, 1966. Phase relations involving sphalerite in the Fe-Zn-S system. Econ. Geol., *61*, 815-849.

Boorman, R. S., 1967. Subsolidus studies in the ZnS-FeS-FeS_2 system. Econ. Geol., *62,* 614-631.

Bragg, W. L., 1913. The analysis of crystals by the X-ray spectrometer. Proc. Royal Soc. London, *89A*, 468-489.

Enjoji, M. and Nedachi, M., 1983. Fluid inclusions in the minerals from the Kano mine, Miyazaki Prefecture (abstr.). Joint Meeting of Soc. Mining Geol. Japan, Assoc. Miner. Petr. Econ. Geol., and Miner. Soc. Japan, C-38. (in Japanese)

Enjoji, M. and Shoji, T., 1981. Fluid inclusion study on the Tsumo skarn-type deposit, southwestern Japan. Mining Geol., *31*, 381-396. (in Japanese with English abstr.)

Imai, H., 1973. Geology and fluid inclusion of the Ashio ore deposit. 1st Abstr. General Research Assemblage (B) 830707, 12-13. (in Japanese)

Ishihara, S., Sato, K. and Tsukimura, K. 1981. Some aspects on the tin-polymetallic veins in the Akenobe mine area, Southwest Japan. Mining Geol., *31*, 147-156. (in Japanese)

Kato, A.,1969. Stannoidite, $Cu_5(Fe,Zn)_2SnS_8$, a new stannite-like mineral from the Konjo, Okayama Prefecture, Japan. Bull. Nat. Sci. Mus. Tokyo, *12*, 165-172.

Kato, A. and Shinohara, K., 1968. The occurrence of roquesite from the Akenobe mine, Hyogo Prefecture, Japan. Miner. Jour., *5*, 276-284.

Kim, M. S., Fujiki, Y., Takenouchi, S. and Imai, H. 1972. Studies on the fluid inclusions in the minerals from the Ohtani and Kaneuchi mines. Mining Geol., *22*, 449-455. (Japanese with English abstr.)

Lee. M. S., Takenouchi, S., and Imai, H., 1975. Syntheses of stannoidite and mawsonite and their geneses in ore deposits. Econ. Geol., *70*, 834-843.

Nakamura, Y., 1983. An example of the mode of occurrence of stannite and sphalerite, based on Fe and Zn partition between them (abstr.). General Research Assemblage on "Research on opaque mineral paragenesis and genesis of its texture (re-examination)", 67-72. (in Japanese)

Nakamura, Y. and Shima, H., 1982. Fe and Zn partitioning between sphalerite and stannite (abstr.). Joint Meeting of Soc. Mining Geol. Japan, Assoc. Miner. Petr. Econ. Geol., and Miner. Soc. Japan, A-8. (in Japanese)

Nekrasov, I. J., Sorokin, V. I. and Osadchii, E. G., 1979. Fe and Zn partitioning between stannite and sphalerite and its application in geothermometry. *In* Origin and Distribution of the Elements, L. H. Ahrens ed., Phys. Chem. Earth, *34*, 739-742.

Nishio, S., Imai, H., Inuzuka, S. and Okada, Y., 1953. Temperatures of mineral formation in some deposits in Japan, as measured by the decrepitation method. Mining Geol., *3*, 21-29. (in Japanese with English abstr.)

Sasaki, A. and Ishihara, S. 1980. Sulphur isotope characteristics of granitoids and related mineral deposits in Japan. Proc. 5th Quart. IAGOD Symp. *1*, 325-335.

Schneeberg, E. P., 1973. Sulfur fugacity measurements with the electrochemical cell $Ag/AgI/Ag_{2+x}S$, $f(S_2)$. Econ. Geol., *68*, 507-517.

Scott, S. D. and Barnes, H. L., 1971. Sphalerite geothermometry and geobarometry. Econ. Geol., *66*, 653-669.

Shimizu, M. and Iiyama, J. T., 1982. Zinc-lead skarn deposits of the Nakatatsu mine, central Japan. Econ. Geol., *77*, 1000-1012.

Shimizu, M. and Kato, A., 1991. Roquesite-bearing tin ores from the Omodani, Akenobe, Fukoku, and Ikuno polymetallic vein-type deposits in the Inner zone of southwestern Japan. Canad. Miner., *29*, 207-215.

Shimizu, M. and Shikazono, N., 1985. Iron and zinc partitioning between coexisting stannite and sphalerite: a possible indicator of temperature and sulfur fugacity. Miner. Deposita, *20*, 314-320.

Shimizu, M. and Shikazono, N., 1987. Stannoidite-bearing tin ore: mineralogy, texture and physicochemical environment of formation. Canad. Miner., *25*, 229-236.

Shiozawa, T., 1983. Mineralization of the Akenobe Tin-Polymetallic Deposits, Hyogo Prefecture, Central Japan, with Special Reference to the Chiemon Vein Swarm. Unpubl. Master's Thesis, Univ. Tokyo.

Takenouchi, S., 1983. Study on fluid inclusions in the minerals from the Kuga tungsten deposits, Yamaguchi Prefecture (abstr.). Joint Meeting of Soc. Mining Geol. Japan, Assoc. Miner. Petr. Econ. Geol., and Miner. Soc. Japan, C-30. (in Japanese)

Takenouchi, S. and Imai, H., 1971. Fluid inclusion study of some tungsten-quartz veins in Japan. Soc. Mining Geol. Japan, Spec. Issue *3*: Proc. IMA-IAGOD Meeting 70, IAGOD Vol., 345-350.

Urashima, Y. and Nedachi, M., 1983. Opaque minerals from the deposits around Suzuyama, Kagoshima Prefecture (abstr.). Joint Meeting of Soc. Mining Geol. Japan, Assoc. Miner. Petr. Econ. Geol., and Miner. Soc. Japan, C-28. (in Japanese)

Yamamoto, M. 1974. Distribution of sulfur isotopes in the Ryusei vein of the Akenobe mine, Hyogo Prefecture, Japan. Geochem. Jour., *8*, 75-86.

Received 5 November 2007; accepted 18 February 2008